

Thermodynamics of Phase and Chemical Equilibrium in a Strongly Nonideal Esterification System

Sascha Grob and Hans Hasse*

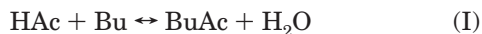
Institute of Thermodynamics and Thermal Process Engineering, University of Stuttgart, D-70550 Stuttgart, Germany

In this study, the reaction equilibrium of the reversible esterification of acetic acid with 1-butanol giving 1-butyl acetate and water was investigated. The entire composition space including the miscibility gap was covered at temperatures relevant for technical processes (353.15 K to 393.15 K). The experiments were carried out in a multiphase batch reactor with online gas chromatography and in a batch reactor with quantitative ^1H NMR spectroscopy, respectively. The thermophysical database available in the literature was complemented by measurements of liquid–liquid and vapor–liquid equilibria. On the basis of that comprehensive data, thermodynamically consistent models of the reaction equilibrium were developed which predict the concentration dependence of the mass action law pseudo-equilibrium constant, K_x . The following different modeling approaches are compared: the G^E models NRTL and UNIQUAC as well as the PC-SAFT equation of state and the COSMO-RS model. All of them can successfully be used, the COSMO-RS model, however, has the highest predictive power.

Introduction

The design of reactive separation processes such as reactive distillation requires reliable thermodynamic models which describe both phase and reaction equilibrium. The phase and chemical equilibrium model should be consistent.¹ The development of such models is often difficult, as suitable reaction data are scarce in most cases. Most studies on reaction equilibrium cover only a small part of the composition space. For example, Lee et al. studied reaction equilibrium of several esterification reactions starting from mixtures which mostly consisted of two components.^{2–4} The broadest investigation concerning reaction equilibrium of esterification systems is that published by Kang et al.⁵ concerning the system ethanol + acetic acid + ethyl acetate + water. Kang et al.⁵ provide reaction equilibrium data for mixtures covering a large part of the composition space but exclude the reaction equilibrium with superposed liquid–liquid equilibrium.

Thermodynamic modeling of reacting multiphase systems is a challenging task which should be based on comprehensive experimental data. On that background, studies on a highly nonideal test system which is of interest in reactive distillation were carried out, the esterification of acetic acid (HAc) with 1-butanol (Bu) to 1-butyl acetate (BuAc) and water (H_2O):



Important experimental studies on the chemical equilibrium of this esterification reaction are those of Leyes and Othmer,⁶ Hirata and Komatsu,⁷ and Zhuchkov.⁸ Furthermore, there exist several experimental studies on reaction kinetics which also provide some information concerning reaction equilibrium. However, none of these studies considers the concentration dependence of reaction equi-

librium over a wide composition space including the miscibility gap.

Materials and Methods

a. Chemicals and Preparation of Samples. Acetic acid, 1-butanol, and 1-butyl acetate were of analytical grade (Bu, 99.8% (GC); HAc, 99.8% (acidmetric); BuAc, 99.5% (GC)). Water was bidistilled. Sulfuric acid (p.a., 96.0%) was selected as catalyst. Mixtures were prepared gravimetrically with an accuracy of 0.001 g and a minimum amount of each reactant of 5.0 g (0.1 g for sulfuric acid).

b. Batch Reactor with Online Gas Chromatography for the Determination of Reaction Equilibrium in Liquid Systems with Limited Miscibility. One part of the experiments was carried out in a 30 cm³ view-cell used as a multiphase batch reactor (see Figure 1). The design is similar to that described by Wendland.⁹ The reactor has two sample loops which allow the analysis of liquid phases also in the case of a phase split. Appropriate positioning of the inlet and outlet of the loops is possible by rotating the cylindrical reactor around its longitudinal axis. For pumping, two low pulsation gear pumps are used in the loops. Samples are taken through an air-actuated valve directly coupled to the feed line of a gas chromatograph. The temperature of the reactor is maintained constant by a liquid thermostated heating jacket to ± 0.2 K. The reactor, the sample loop, and the sampling valves are located in an air-heated glass cabinet. The temperature in the glass cabinet typically exceeds the temperature in the heating jacket by (2 to 5) K. As the mutual solubility of the organic and the aqueous liquid phase increases with increasing temperature, the liquid phase circulating in the loop does not split. As the investigated mixture contains sulfuric acid and acetic acid at temperatures up to 393 K, the apparatus has to be resistant against corrosion. Therefore, the reactor, the tubing, and the sample valve consist of Hastelloy C. As corrosion-resistant and at the same time pulsation-free pumps were not available, stainless steel gear pumps were

* Corresponding author. Phone: +49-711-685-6105. Fax: +49-711-685-7657. E-mail: hasse@itt.uni-stuttgart.de.

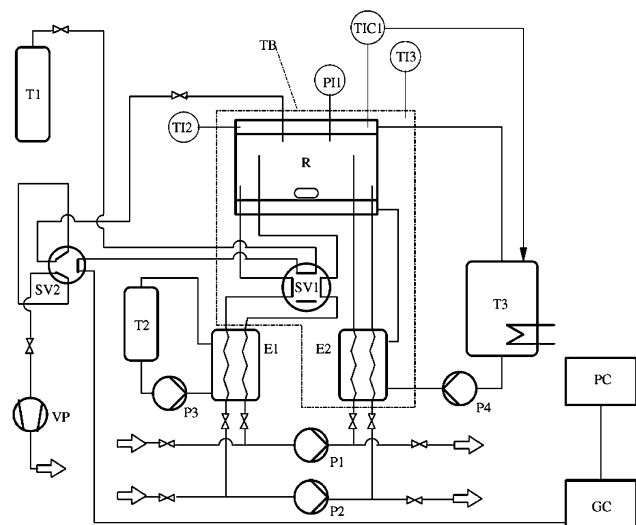


Figure 1. Apparatus for measuring multiphase reaction equilibria. E1, sample water cooler; E2, sample heater; GC, gas chromatograph; P1, sample loop pump (light phase); P2, sample loop pump (heavy phase); P3, cooling water pump; P4, heating oil pump; PC, computer; P11, pressure sensor; R, batch reactor; SV1, sample valve (liquid phases); SV2, sample valve (vapor phase); T1, helium cylinder; T2, cooling water tank; T3, heater tank with temperature control; TB, thermostated glass box; TIC1, platinum resistance thermometer (input of temperature control of T3); TI2, platinum resistance thermometer; TI3, thermoelement; VP, vacuum pump.

used. To avoid corrosion of the pumps, the liquid in the sample loops is cooled before entering the pump. The sample passes the valve before entering the cooler so that no problems with sampling occur. After passing the pump, the sample is again heated to the temperature in the reactor.

Gas chromatographic analysis was carried out with a Hewlett-Packard GC (HP 5890A) equipped with a Chrom-pack CP52B column and a thermal conductivity detector. A temperature program (60 °C to 180 °C) was used. From calibration which was based on binary, ternary, and quaternary mixtures, linear response factors describing the relation between signal areas and composition were determined. The accuracy of the mole fractions is typically better than 4% (relative deviation). For small peaks (relative signal area below ~ 0.05), the error may rise to 25% (relative deviation). The corresponding numbers for the repeatability of the analytical results are lower by a factor of ~ 2 . The mole fractions given in the tables given below are mean values of three or more measurements. For more details, see Grob.¹⁰

c. NMR Flow Cell for the Determination of Reaction Equilibrium in Homogeneous Liquid Systems. Reaction equilibria were also studied by ^1H NMR spectroscopy. The experiments were carried out in a 95 μL NMR flow cell used as a batch reactor. For details on the experimental method, see Maiwald et al.¹¹ Figure 2 shows a typical ^1H NMR spectrum of a reacting mixture of 1-butanol, acetic acid, 1-butyl acetate, and water. The composition of a sample is calculated from the initial composition and the signals *D* and *d* which are caused by protons in 1-butyl acetate and 1-butanol, respectively. These are the only two signals which are caused by protons in single components. The area below these signals is directly proportional to the number of corresponding molecules. As the proportionality constants are the same for both signals, no calibration is necessary. The signal of the OH groups shifts strongly with varying composition of the mixture and may overlap with

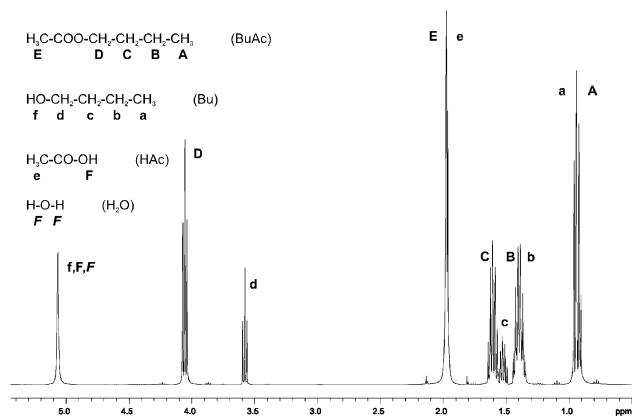


Figure 2. Typical ^1H NMR spectrum of a reacting mixture of water + 1-butyl acetate + 1-butanol + acetic acid.

one of the signals, *D* or *d*, so that the corresponding spectrum cannot be evaluated. The accuracy of mole fractions calculated from ^1H NMR spectroscopic data is typically better than 5% (relative deviation), and the repeatability is usually better than 2%. The main advantage of ^1H NMR spectroscopy over gas chromatography is that at similar accuracy the time needed to acquire a ^1H NMR spectrum is only ~ 10 s whereas the acquisition of a gas chromatogram takes ~ 20 min. The experiments carried out with NMR spectroscopy are marked in the tables given below. In all other cases, analysis was carried out using gas chromatography.

d. Experiments on Liquid–Liquid Equilibrium. The batch reactor with online gas chromatography described above was also used for the investigation of binary and ternary liquid–liquid equilibrium under conditions where chemical reactions are negligible. The numbers given there for accuracy and repeatability also hold for the results for each phase in liquid–liquid equilibrium measurements.

e. Experiments on Vapor–Liquid Equilibrium. Experiments on vapor–liquid equilibrium were carried out in a circulating still.¹² In experiments concerning reactive subsystems (subsystems containing both butanol and acetic acid), reaction I cannot be totally avoided using a circulating still because acetic acid catalyzes both the esterification reaction and the hydrolysis of the ester. However, the autocatalyzed reaction is slow compared to the time needed to reach the vapor–liquid equilibrium. Analysis was done by gas chromatography (see above).

The uncertainty of the experiments is higher than the uncertainty of vapor–liquid equilibrium experiments on nonreactive mixtures: for the temperature, the uncertainty is ~ 0.6 K; for the mole fractions, it is < 0.02 (absolute deviation). The repeatability is again better than the numbers given above.

Modeling

Phase equilibrium is usually modeled using either G^E models or equations of state. Employing G^E models, phase equilibrium is described here by

$$p_i^S(T)x_i\gamma_i(T, \underline{x}) = py_i \quad (1)$$

where p_i^S is the vapor pressure of component *i*, x_i , the mole fraction of component *i* in the liquid phase, γ_i , the activity coefficient of component *i* in the liquid phase, y_i , the mole fraction of component *i* in the vapor phase, *p*, the pressure, and *T*, the temperature.

Analogously, liquid–liquid equilibrium between the phases prime and double prime is described by

$$x_i' \gamma_i'(T, \underline{x}') = x_i'' \gamma_i''(T, \underline{x}'') \quad (2)$$

If an equation of state is used, both vapor–liquid and liquid–liquid equilibrium are described by

$$x_i' \varphi_i'(T, \underline{x}') = x_i'' \varphi_i''(T, \underline{x}'') \quad (3)$$

where φ_i is the fugacity coefficient of component i and prime and double prime mark the two phases in equilibrium.

The reaction equilibrium of reaction I is modeled either with the activity-based reaction equilibrium constant

$$K_a(T) = K_x(T, \underline{x}) K_\gamma(T, \underline{x}) = \frac{x_{\text{BuAc}} x_{\text{H}_2\text{O}} \gamma_{\text{BuAc}} \gamma_{\text{H}_2\text{O}}}{x_{\text{Bu}} x_{\text{HAc}} \gamma_{\text{Bu}} \gamma_{\text{HAc}}} \quad (4)$$

or with the fugacity-based reaction equilibrium constant

$$K_f(T) = K_x(T, \underline{x}) K_\varphi(T, \underline{x}) = \frac{x_{\text{BuAc}} x_{\text{H}_2\text{O}} \varphi_{\text{BuAc}} \varphi_{\text{H}_2\text{O}}}{x_{\text{Bu}} x_{\text{HAc}} \varphi_{\text{Bu}} \varphi_{\text{HAc}}} \quad (5)$$

The influence of pressure on the reaction can be neglected here. Both K_a and K_f only depend on temperature but not on mixture composition. Thus, the composition dependence of K_γ or K_φ , respectively, cancels the concentration dependence of K_x .

Both constants are linked by

$$\frac{K_f}{K_a} = \frac{K_\varphi}{K_\gamma} = \frac{p_{\text{BuAc}}^{\text{S}} p_{\text{H}_2\text{O}}^{\text{S}}}{p} \frac{p}{p_{\text{Bu}}^{\text{S}} p_{\text{HAc}}^{\text{S}}} = \frac{p_{\text{BuAc}}^{\text{S}} p_{\text{H}_2\text{O}}^{\text{S}}}{p_{\text{Bu}}^{\text{S}} p_{\text{HAc}}^{\text{S}}} = K_{p_i^{\text{S}}} \quad (6)$$

Simultaneous modeling of phase and reaction equilibrium has recently been discussed by Hasse¹ and Ott and Hasse.¹³ The basic question of thermodynamic modeling of reaction equilibrium over a wide concentration range is whether the concentration dependence of K_x (or K_γ or K_φ , respectively) can reliably be predicted by the studied thermodynamic models.

In the present work, four thermodynamic models are used: the G^{E} models NRTL¹⁴ and UNIQUAC,¹⁵ the PC-SAFT equation of state,^{16,17} and the COSMO-RS model.¹⁸

The PC-SAFT equation of state is a modification of the SAFT equation of state and is based on Wertheim's perturbation theory using a fluid of chains of hard spheres as reference fluid. It was developed for the modeling of associating fluids. The PC-SAFT equation of state uses only one binary parameter per binary mixture, whereas UNIQUAC and NRTL use two or three binary parameters, respectively.

COSMO-RS distinguishes a combinatorial and a residual contribution to the behavior of real solvents. The combinatorial part is modeled empirically and does not include any binary parameters. The model of the residual part is based on the idea that a mixture of interacting molecules corresponds to a mixture of interacting surface segments. The starting point of the COSMO-RS model is single molecules which are situated in a cavity inside a conductor. The surface charge density distribution of a molecule in the conductor is calculated from quantum mechanics using density functional theory. In a mixture, the surface segments of the molecules interact, and electrostatic interaction energy is considered. Thus, COSMO-RS treats a system of molecules as an ensemble of interacting surface segments. Using methods of statistical thermodynamics,

Table 1. Liquid–Liquid Equilibria in the Binary System Water + 1-Butyl Acetate

$t/^\circ\text{C}$	$x'_{\text{H}_2\text{O}}$	$x''_{\text{H}_2\text{O}}$	$t/^\circ\text{C}$	$x'_{\text{H}_2\text{O}}$	$x''_{\text{H}_2\text{O}}$
75.0	0.092	0.995	105.0	0.146	0.994
80.0	0.118	0.997	110.0	0.166	0.991
85.0	0.102	0.990	115.0	0.200	0.985
90.0	0.129	0.994	120.0	0.210	0.990
95.0	0.125	0.992	125.0	0.213	0.994
100.0	0.150	0.993			

Table 2. Liquid–Liquid Equilibria in the Ternary System Water + 1-Butyl Acetate + 1-Butanol

$t/^\circ\text{C}$	$x'_{\text{H}_2\text{O}}$	x'_{BuAc}	x'_{Bu}	$x''_{\text{H}_2\text{O}}$	x''_{BuAc}	x''_{Bu}
80.0	0.125	0.792	0.083	0.994	0.003	0.003
	0.196	0.602	0.202	0.992	0.002	0.006
	0.288	0.409	0.303	0.988	0.003	0.009
	0.386	0.233	0.381	0.985	0.002	0.013
	0.503	0.080	0.417	0.982	0.001	0.017
100.0	0.169	0.762	0.069	0.989	0.008	0.003
	0.220	0.587	0.193	0.988	0.005	0.007
	0.319	0.387	0.294	0.981	0.006	0.012
	0.432	0.209	0.359	0.982	0.003	0.015
	0.570	0.064	0.366	0.977	0.002	0.021
120.0	0.267	0.578	0.155	0.990	0.005	0.005
	0.346	0.401	0.253	0.982	0.006	0.012
	0.591	0.095	0.314	0.971	0.003	0.026
	0.473	0.191	0.336	0.979	0.003	0.018
	0.241	0.626	0.133	0.985	0.009	0.006

Table 3. Liquid–Liquid Equilibria in the Pseudoternary System Water + 1-Butyl Acetate + Acetic Acid

$t/^\circ\text{C}$	$x'_{\text{H}_2\text{O}}$	x'_{BuAc}	x'_{Bu}	$x''_{\text{H}_2\text{O}}$	x''_{BuAc}	x''_{Bu}
80.0	0.121	0.858	0.004	0.990	0.002	0.000
	0.169	0.743	0.015	0.971	0.004	0.001
	0.245	0.622	0.003	0.935	0.005	0.000
	0.340	0.462	0.012	0.897	0.008	0.002
	0.517	0.241	0.019	0.817	0.026	0.008
100.0	0.179	0.786	0.005	0.980	0.006	0.000
	0.261	0.659	0.003	0.945	0.016	0.001
	0.375	0.457	0.007	0.901	0.013	0.002
	0.433	0.362	0.007	0.873	0.014	0.003
	0.498	0.281	0.009	0.841	0.021	0.005
120.0	0.256	0.706	0.011	0.966	0.019	0.001
	0.337	0.564	0.015	0.947	0.008	0.002
	0.427	0.416	0.015	0.908	0.008	0.004
	0.556	0.241	0.017	0.843	0.022	0.010
	0.572	0.228	0.014	0.837	0.030	0.009

the overall interaction energy of the mixture is calculated. COSMO-RS uses some empirical terms in the combinatorial part and for modeling H-bonds and van der Waals forces. These are, however, universal and do not depend on the studied system. Furthermore, one parameter per chemical element is required. COSMO-RS, hence, does not use any parameters which are fitted to the physical properties of the studied mixture.

Experimental Phase Equilibria

a. Liquid–Liquid Equilibria. Experiments on ternary and quaternary liquid–liquid equilibria were carried out at temperatures between 353.15 K and 393.15 K. Furthermore, liquid–liquid equilibria in the binary system water + 1-butyl acetate were studied. The experimental results are given in Tables 1–4. Additional information on liquid–liquid equilibria in the reacting quaternary system is given in Table 11. Since acetic acid does not only take part in the esterification but also acts as a catalyst, reaction I cannot be totally avoided in ternary mixtures containing acetic acid. As the autocatalyzed reaction is slow compared to the time needed to reach the liquid–liquid equilibrium, the concentration of the fourth component is always smaller than 0.02 mol/mol. The results can be presented

Table 4. Liquid–Liquid Equilibria in the Pseudoternary System Water + 1-Butanol + Acetic Acid

$t/^\circ\text{C}$	$x'_{\text{H}_2\text{O}}$	x'_{BuAc}	x'_{Bu}	$x''_{\text{H}_2\text{O}}$	x''_{BuAc}	x''_{Bu}
80.0	0.646	0.002	0.336	0.973	0.000	0.024
	0.718	0.002	0.252	0.960	0.000	0.030
	0.746	0.001	0.222	0.952	0.000	0.035
	0.785	0.002	0.180	0.906	0.001	0.074
100.0	0.716	0.001	0.275	0.971	0.000	0.027
	0.747	0.001	0.240	0.964	0.000	0.034
	0.765	0.001	0.223	0.966	0.000	0.030
	0.785	0.002	0.199	0.960	0.000	0.034

Table 5. Vapor–Liquid Equilibria in the Pseudobinary System 1-Butanol + Acetic Acid

$t/^\circ\text{C}$	$x_{\text{H}_2\text{O}}$	x_{BuAc}	x_{Bu}	$y_{\text{H}_2\text{O}}$	y_{BuAc}	y_{Bu}
$p = 30 \text{ kPa}$						
82.82	0.0055	0.0003	0.0427	0.0124	0.0002	0.0229
85.79	0.0031	0.0013	0.1898	0.0076	0.0014	0.1196
88.56	0.0037	0.0013	0.3616	0.0096	0.0017	0.2846
90.34	0.0018	0.0010	0.6352	0.0065	0.0017	0.6376
90.09	0.0013	0.0003	0.7230	0.0047	0.0006	0.7585
89.61	0.0012	0.0002	0.7930	0.0045	0.0004	0.8431
88.09	0.0000	0.0002	0.9257	0.0031	0.0004	0.9601
$p = 50 \text{ kPa}$						
97.07	0.0049	0.0006	0.0463	0.0088	0.0005	0.0301
99.85	0.0038	0.0029	0.1961	0.0080	0.0030	0.1430
101.74	0.0042	0.0027	0.3600	0.0135	0.0034	0.2951
102.96	0.0032	0.0024	0.4972	0.0077	0.0031	0.4725
103.02	0.0027	0.0018	0.6310	0.0082	0.0026	0.6459
102.78	0.0019	0.0010	0.7186	0.0041	0.0014	0.7491
102.09	0.0012	0.0004	0.7855	0.0043	0.0007	0.8418
101.15	0.0019	0.0005	0.8669	0.0055	0.0008	0.9126
100.64	0.0000	0.0003	0.9203	0.0020	0.0004	0.9519
$p = 70 \text{ kPa}$						
106.83	0.0050	0.0012	0.0446	0.0111	0.0011	0.0284
109.41	0.0047	0.0054	0.1993	0.0118	0.0056	0.1477
110.94	0.0056	0.0049	0.3557	0.0192	0.0058	0.3010
112.10	0.0028	0.0027	0.6233	0.0070	0.0035	0.6424
110.94	0.0014	0.0008	0.7822	0.0046	0.0011	0.8405
109.64	0.0016	0.0003	0.8705	0.0073	0.0004	0.9210
109.30	0.0000	0.0004	0.9165	0.0020	0.0005	0.9488
$p = 90 \text{ kPa}$						
114.53	0.0060	0.0021	0.0420	0.0134	0.0019	0.0280
116.73	0.0062	0.0084	0.1928	0.0174	0.0086	0.1458
118.40	0.0070	0.0074	0.3552	0.0193	0.0085	0.3148
119.15	0.0053	0.0060	0.4897	0.0146	0.0073	0.4763
119.13	0.0031	0.0038	0.6209	0.0092	0.0049	0.6439
118.63	0.0020	0.0030	0.7001	0.0072	0.0041	0.7465
117.82	0.0020	0.0013	0.7822	0.0059	0.0017	0.8413
116.78	0.0019	0.0005	0.8639	0.0053	0.0006	0.9127
116.08	0.0000	0.0005	0.9131	0.0023	0.0006	0.9495

Table 6. Vapor–Liquid Equilibria in the Pseudoternary System Water + 1-Butanol + Acetic Acid

$t/^\circ\text{C}$	$x_{\text{H}_2\text{O}}$	x_{BuAc}	x_{Bu}	$y_{\text{H}_2\text{O}}$	y_{BuAc}	y_{Bu}
$p = 40 \text{ kPa}$						
82.96	0.2421	0.0005	0.3981	0.5339	0.0005	0.2523
90.15	0.0804	0.0003	0.7834	0.3014	0.0003	0.6370
88.22	0.1034	0.0006	0.1471	0.2043	0.0007	0.0919
73.07	0.7912	0.0001	0.0871	0.9369	0.0001	0.0371
78.94	0.4311	0.0004	0.1929	0.6524	0.0005	0.1294
79.45	0.3485	0.0003	0.4188	0.6314	0.0003	0.2600
86.63	0.1795	0.0005	0.4068	0.4041	0.0006	0.2878
$p = 70 \text{ kPa}$						
103.79	0.0761	0.0004	0.7848	0.2676	0.0005	0.6666
103.88	0.0926	0.0014	0.1501	0.1986	0.0015	0.1010
86.89	0.7877	0.0001	0.0826	0.8431	0.0004	0.1163
92.82	0.4162	0.0008	0.1944	0.6559	0.0010	0.1371
93.10	0.3397	0.0005	0.4213	0.6241	0.0005	0.2701
100.92	0.1647	0.0011	0.4090	0.4106	0.0013	0.2930

in pseudoternary phase diagrams which are deduced using the transformation of quaternary compositions into pseudoternary compositions with the help of the method described

Table 7. Vapor–Liquid Equilibria in the Pseudoternary System 1-Butyl Acetate + 1-Butanol + Acetic Acid

$t/^\circ\text{C}$	$x_{\text{H}_2\text{O}}$	x_{BuAc}	x_{Bu}	$y_{\text{H}_2\text{O}}$	y_{BuAc}	y_{Bu}
$p = 40 \text{ kPa}$						
95.06	0.0012	0.2798	0.3938	0.0049	0.3171	0.3866
94.43	0.0000	0.1004	0.7692	0.0055	0.1389	0.7824
93.35	0.0026	0.0992	0.1539	0.0067	0.0925	0.1056
95.19	0.0000	0.7201	0.1009	0.0055	0.6902	0.1245
94.71	0.0020	0.3927	0.2068	0.0068	0.3922	0.1953
94.40	0.0000	0.3779	0.3926	0.0041	0.4098	0.4057
95.59	0.0000	0.1909	0.4133	0.0043	0.2251	0.3904
$p = 70 \text{ kPa}$						
110.53	0.0017	0.2836	0.3889	0.0056	0.3037	0.3979
109.19	0.0000	0.1008	0.7592	0.0045	0.1244	0.7899
109.27	0.0027	0.1001	0.1537	0.0073	0.0941	0.1162
111.67	0.0000	0.7293	0.0951	0.0043	0.6909	0.1203
110.67	0.0016	0.3975	0.2032	0.0051	0.3868	0.2035
110.08	0.0000	0.3821	0.3808	0.0032	0.3925	0.4090
110.95	0.0016	0.1937	0.4069	0.0048	0.2151	0.4014

Table 8. Vapor–Liquid Equilibria in the Quaternary System Water + 1-Butyl Acetate + 1-Butanol + Acetic Acid

$t/^\circ\text{C}$	$x_{\text{H}_2\text{O}}$	x_{BuAc}	x_{Bu}	$y_{\text{H}_2\text{O}}$	y_{BuAc}	y_{Bu}
$p = 40 \text{ kPa}$						
86.18	0.1558	0.2732	0.2845	0.3392	0.2448	0.2149
86.68	0.0704	0.2927	0.3149	0.3190	0.2558	0.2207
$p = 70 \text{ kPa}$						
99.45	0.1053	0.2880	0.2973	0.3743	0.2326	0.2085
103.90	0.0549	0.2971	0.3174	0.2393	0.2648	0.2572

Table 9. Vapor–Liquid Equilibria in the System 1-Butyl Acetate + Acetic Acid (Previously Unpublished Data by Kuranov²¹)

$t/^\circ\text{C}$	x_{BuAc}	y_{BuAc}	$t/^\circ\text{C}$	x_{BuAc}	y_{BuAc}	$t/^\circ\text{C}$	x_{BuAc}	y_{BuAc}
$p = 20 \text{ kPa}$			$p = 50 \text{ kPa}$			$p = 90 \text{ kPa}$		
72.04	0.000	0.000	96.09	0.000	0.000	113.86	0.000	0.000
72.22	0.027	0.020	96.30	0.027	0.023	114.08	0.025	0.024
72.51	0.058	0.036	96.58	0.049	0.039	114.60	0.075	0.051
73.12	0.124	0.082	97.41	0.144	0.111	115.22	0.144	0.101
74.18	0.239	0.170	98.21	0.237	0.172	116.12	0.227	0.172
75.11	0.333	0.245	99.08	0.328	0.255	117.10	0.304	0.241
75.68	0.415	0.325	100.00	0.421	0.344	118.00	0.400	0.320
76.26	0.492	0.405	100.50	0.486	0.411	118.18	0.422	0.348
76.93	0.576	0.510	101.08	0.553	0.494	119.42	0.560	0.501
77.47	0.688	0.632	101.64	0.657	0.612	120.16	0.672	0.617
77.93	0.781	0.743	102.33	0.770	0.741	120.87	0.770	0.724
78.36	0.950	0.942	103.00	0.942	0.939	121.90	0.939	0.936
78.41	1.000	1.000	103.22	1.000	1.000	122.24	1.000	1.000

by Ung and Doherty.¹⁹ However, in Tables 3 and 4, the measured concentrations are directly reported. The mole fractions of the fourth component result from $\sum x_i = 1$. The same holds for Tables 5–8 and 11.

Figure 3 shows the liquid–liquid equilibrium in the ternary system water + 1-butyl acetate + 1-butanol at 353.15 K, 373.15 K, and 393.15 K. Figure 4 shows the results for the pseudoternary system water + 1-butyl acetate + acetic acid. In Figure 5, the liquid–liquid equilibria in the pseudoternary system water + 1-butanol + acetic acid are shown at 353.15 K and 373.15 K. Figure 6 shows the reactive liquid–liquid equilibrium in the quaternary system water + 1-butyl acetate + 1-butanol + acetic acid at 353.15 K, 373.15 K, and 393.15 K using transformed pseudoternary composition according to Ung and Doherty¹⁹ applied to the ester hydrolysis. In that presentation, the true composition of the quaternary mixture is stoichiometrically transformed into a pseudoternary system which contains only one of the components 1-butanol or acetic acid. The two resulting triangular diagrams (one for 1-butanol as the third component and

Table 10. Chemical Equilibrium Data for Reaction I in the System Water + 1-Butyl Acetate + 1-Butanol + Acetic Acid in the Homogeneous Liquid Phase

$t/^\circ\text{C}$	$x_{\text{H}_2\text{O}}$	x_{BuAc}	x_{Bu}	x_{HAc}	K_x	analysis	$t/^\circ\text{C}$	$x_{\text{H}_2\text{O}}$	x_{BuAc}	x_{Bu}	x_{HAc}	K_x	analysis
80.0	0.292	0.402	0.159	0.147	5.0	GC	100.0	0.362	0.098	0.010	0.530	6.5	GC
	0.102	0.180	0.708	0.010	2.7	GC		0.520	0.087	0.019	0.374	6.5	GC
	0.085	0.358	0.539	0.018	3.1	GC		0.701	0.076	0.035	0.188	8.0	GC
	0.074	0.538	0.364	0.024	4.5	GC		0.328	0.275	0.038	0.359	6.6	GC
	0.062	0.705	0.198	0.035	6.2	GC		0.307	0.247	0.413	0.033	5.6	GC
	0.021	0.845	0.056	0.078	4.1	GC		0.140	0.156	0.694	0.010	3.1	GC
	0.053	0.711	0.033	0.203	5.7	GC		0.203	0.229	0.541	0.027	3.2	GC
	0.071	0.556	0.015	0.358	7.5	GC		0.148	0.157	0.684	0.011	3.0	GC
	0.086	0.386	0.007	0.521	9.2	GC		0.206	0.223	0.543	0.028	3.0	GC
	0.178	0.557	0.132	0.133	5.6	GC		0.133	0.275	0.579	0.013	4.9	GC
	0.100	0.696	0.106	0.098	6.7	GC		0.125	0.199	0.653	0.023	1.7	GC
	0.181	0.393	0.386	0.040	4.6	GC		0.131	0.237	0.612	0.020	2.5	GC
	0.196	0.424	0.031	0.349	7.8	GC		0.094	0.194	0.006	0.706	4.4	NMR
	0.381	0.288	0.177	0.154	4.0	GC		0.027	0.827	0.073	0.073	4.3	NMR
	0.190	0.097	0.705	0.008	3.4	GC		0.184	0.516	0.150	0.150	4.2	NMR
	0.342	0.078	0.563	0.017	2.9	GC		0.076	0.696	0.114	0.114	4.1	NMR
	0.352	0.092	0.009	0.547	6.4	GC		0.163	0.353	0.027	0.457	4.7	NMR
	0.518	0.083	0.020	0.379	5.5	GC		0.387	0.287	0.163	0.163	4.2	NMR
	0.691	0.073	0.040	0.196	6.5	GC		0.355	0.165	0.025	0.455	5.2	NMR
	0.485	0.078	0.407	0.030	3.1	GC		0.196	0.096	0.004	0.704	6.1	NMR
0.316	0.282	0.041	0.361	6.0	GC	0.086	0.386	0.014	0.514	4.5	NMR		
0.308	0.240	0.418	0.034	5.2	GC	0.528	0.194	0.139	0.139	5.3	NMR		
0.095	0.195	0.005	0.705	5.0	NMR	0.344	0.154	0.466	0.036	3.2	NMR		
0.066	0.516	0.384	0.034	2.7	NMR	0.523	0.073	0.377	0.027	3.8	NMR		
0.027	0.827	0.073	0.073	4.2	NMR	0.317	0.391	0.149	0.143	5.8	GC		
0.076	0.526	0.024	0.374	4.5	NMR	0.106	0.186	0.699	0.009	3.1	GC		
0.077	0.697	0.113	0.113	4.2	NMR	0.163	0.556	0.147	0.134	4.6	GC		
0.163	0.353	0.027	0.457	4.8	NMR	0.358	0.277	0.186	0.179	3.0	GC		
0.195	0.095	0.005	0.705	5.3	NMR	0.022	0.869	0.061	0.048	6.6	GC		
0.355	0.165	0.025	0.455	5.2	NMR	0.055	0.581	0.018	0.346	5.2	GC		
0.085	0.385	0.015	0.515	4.4	NMR	0.087	0.209	0.011	0.693	2.4	GC		
100.0	0.303	0.400	0.152	0.145	5.5	GC	0.176	0.103	0.011	0.710	2.3	GC	
	0.101	0.183	0.707	0.009	2.9	GC	0.093	0.530	0.365	0.012	11.2	GC	
	0.083	0.358	0.536	0.023	2.4	GC	0.094	0.194	0.006	0.706	4.4	NMR	
	0.075	0.538	0.359	0.028	4.0	GC	0.027	0.827	0.073	0.073	4.2	NMR	
	0.063	0.692	0.209	0.036	5.7	GC	0.184	0.516	0.150	0.150	4.2	NMR	
	0.033	0.840	0.052	0.075	7.2	GC	0.076	0.696	0.114	0.114	4.0	NMR	
	0.058	0.728	0.032	0.182	7.2	GC	0.162	0.352	0.028	0.458	4.4	NMR	
	0.068	0.560	0.015	0.357	7.2	GC	0.387	0.287	0.163	0.163	4.2	NMR	
	0.077	0.376	0.010	0.537	5.2	GC	0.353	0.163	0.027	0.457	4.8	NMR	
	0.179	0.514	0.155	0.152	3.9	GC	0.195	0.095	0.005	0.705	4.9	NMR	
	0.100	0.697	0.104	0.099	6.8	GC	0.085	0.385	0.015	0.515	4.4	NMR	
	0.169	0.403	0.390	0.038	4.6	GC	0.528	0.078	0.022	0.372	5.0	NMR	
	0.208	0.432	0.029	0.331	9.4	GC	0.525	0.191	0.142	0.142	5.0	NMR	
0.424	0.294	0.157	0.125	6.3	GC	0.518	0.068	0.382	0.032	2.9	NMR		
0.191	0.100	0.702	0.007	4.0	GC								

one for acetic acid as the third component) are joined together along their common axis water + 1-butyl acetate.

b. Vapor–Liquid Equilibria. In the frame of this work, a few experiments on vapor–liquid equilibrium in the reactive quaternary system as well as in the reactive subsystems 1-butanol + acetic acid, water + 1-butanol + acetic acid, and 1-butyl acetate + 1-butanol + acetic acid were carried out in a circulating still, as discussed above. The experimental data on vapor–liquid equilibrium are given in Tables 5–8.

Experimental Reaction Equilibrium

The equilibrium of reaction I was investigated at 353.15 K, 373.15 K, and 393.15 K. The experiments included reaction equilibrium in the miscibility gap. The experimental results of the reaction equilibrium are given in Tables 10 and 11. As a result of the experimental uncertainties, the cumulative uncertainty of the experimental values of the pseudoreaction equilibrium constant

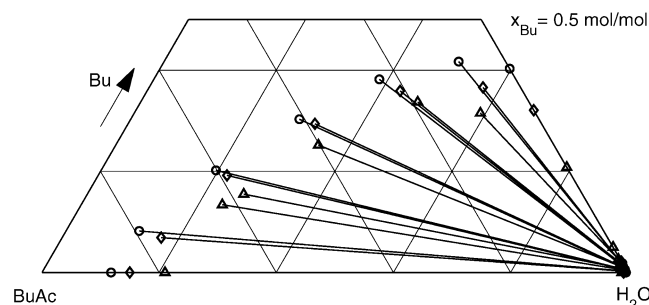
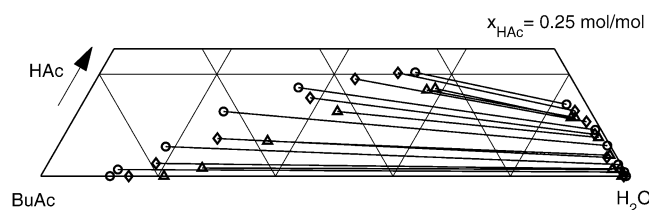
$$K_x = \frac{x_{\text{BuAc}}x_{\text{H}_2\text{O}}}{x_{\text{HAc}}x_{\text{Bu}}} \quad (7)$$

depends on the composition of the considered mixture: If the compositions of all components have the same order of magnitude, the cumulative uncertainty of K_x is <20%. In regions where several components are dilute, distinctly larger cumulative errors may occur. This is in particular the case in the region of the miscibility gap where the cumulative error may reach 100%. The repeatability of the experimental results for K_x is much better; relative deviations are of the order of (2 to 8)% in most cases.

Figure 7 exemplarily shows the results at 373.15 K using transformed pseudoternary composition according to Ung and Doherty¹⁹ applied to the esterification reaction. In the area of the homogeneous liquid phase, clear trends can be observed: The pseudoequilibrium constant, K_x , has the smallest values in mixtures with high concentrations of 1-butanol. K_x increases upon the addition of any of the other three components. This trend is clearer for mixtures containing relatively high amounts of water or 1-butyl acetate, whereas mixtures which are rich in acetic acid have comparatively smaller values of K_x . In the region of liquid–liquid equilibrium, moderate values for K_x are observed in the organic phase, whereas, in the water-rich phase, the values for K_x steeply increase in the direction of pure water. The uncertainty in K_x increases with

Table 11. Chemical Equilibrium Data for Reaction I in the System Water + 1-Butyl Acetate + 1-Butanol + Acetic Acid in Liquid–Liquid Equilibria

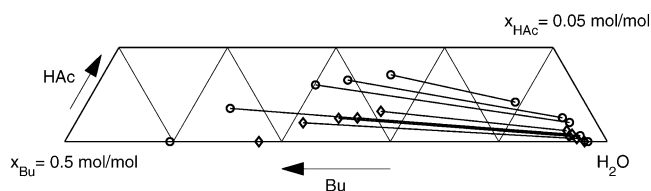
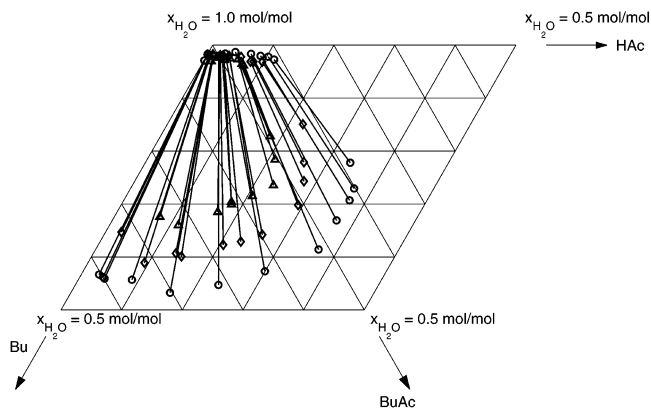
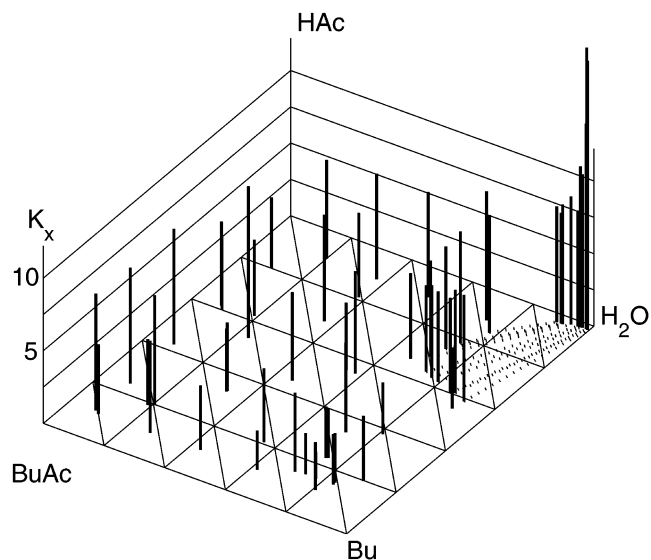
$t/^\circ\text{C}$	$x'_{\text{H}_2\text{O}}$	x'_{BuAc}	x'_{Bu}	K'_x	$x''_{\text{H}_2\text{O}}$	x''_{BuAc}	x''_{Bu}	K''_x
80.0	0.561	0.023	0.410	4.9	0.9707	0.0002	0.0287	19.5
	0.542	0.073	0.370	7.0	0.9782	0.0009	0.0182	19.4
	0.491	0.121	0.346	4.1	0.9687	0.0011	0.0197	5.2
	0.485	0.174	0.279	4.9	0.9632	0.0031	0.0169	10.7
	0.489	0.215	0.212	5.9	0.9587	0.0032	0.0126	9.7
	0.501	0.255	0.131	8.6	0.9465	0.0032	0.0096	7.8
	0.518	0.219	0.112	6.7	0.9178	0.0057	0.0107	7.4
	0.538	0.203	0.090	7.1	0.8990	0.0081	0.0120	7.5
	0.550	0.188	0.082	7.0	0.8845	0.0092	0.0128	6.8
	0.593	0.153	0.069	7.1	0.8712	0.0134	0.0138	8.3
100.0	0.575	0.104	0.289	6.4	0.9731	0.0018	0.0167	12.7
	0.714	0.087	0.062	7.3	0.8839	0.0128	0.0186	7.2
	0.570	0.074	0.337	6.6	0.9765	0.0012	0.0185	16.7
	0.575	0.169	0.133	5.9	0.9268	0.0067	0.0153	7.9
	0.564	0.111	0.288	5.9	0.9757	0.0016	0.0159	17.4
	0.556	0.159	0.212	5.7	0.9565	0.0041	0.0158	10.0
	0.561	0.144	0.233	5.6	0.9617	0.0028	0.0165	9.5
	0.550	0.169	0.189	5.3	0.9472	0.0042	0.0159	7.2
	0.612	0.148	0.109	6.3	0.9028	0.0109	0.0195	7.4
	0.648	0.129	0.092	6.9	0.8970	0.0115	0.0199	6.9
120.0	0.630	0.084	0.256	6.8	0.9601	0.0049	0.0268	21.3
	0.637	0.118	0.182	6.6	0.9544	0.0037	0.0185	8.2
	0.634	0.132	0.133	6.2	0.9259	0.0075	0.0189	7.7
	0.656	0.055	0.269	6.7	0.9740	0.0013	0.0200	13.5
	0.732	0.085	0.087	7.4	0.9046	0.0129	0.0253	8.1
	0.641	0.116	0.180	6.6	0.9455	0.0055	0.0215	9.5
	0.629	0.110	0.205	6.0	0.9562	0.0036	0.0200	9.6
	0.633	0.126	0.159	6.1	0.9380	0.0052	0.0204	6.5
	0.680	0.107	0.109	6.4	0.9100	0.0111	0.0243	7.6

**Figure 3.** Liquid–liquid equilibria in the ternary system water + 1-butyl acetate + 1-butanol: \circ , 353.15 K; \diamond , 373.15 K; \triangle , 393.15 K.**Figure 4.** Liquid–liquid equilibria in the pseudoternary system water + 1-butyl acetate + acetic acid: \circ , 353.15 K; \diamond , 373.15 K; \triangle , 393.15 K.

decreasing concentration of the diluted components. Nevertheless, trends can be clearly discerned. The dependence of reaction equilibrium on temperature is only moderate (see Tables 10 and 11). The trends in the concentration dependence of K_x are the same for all studied temperatures.

Modeling Results

The experimental results from the present work were modeled with the four models mentioned above. The parameters of the NRTL, UNIQUAC, and PC-SAFT models were adjusted to phase equilibrium data. Those data were mostly taken from the Dortmund Datenbank²⁰ and

**Figure 5.** Liquid–liquid equilibria in the pseudoternary system water + 1-butanol + acetic acid: \circ , 353.15 K; \diamond , 373.15 K.**Figure 6.** Liquid–liquid equilibria in the quaternary system water + 1-butyl acetate + 1-butanol + acetic acid: \circ , 353.15 K; \diamond , 373.15 K; \triangle , 393.15 K.**Figure 7.** Experimental pseudoreaction equilibrium constant in the system water + 1-butyl acetate + 1-butanol + acetic acid at 373.15 K: —, experimental K_x ; \cdots , experimental conodes.**Table 12. Pure Component Vapor Pressure Correlations, $\ln(p_i^S(T)/\text{bar}) = A_i + (B_i)/(T/K) + C_i \ln(T/K) + D_i(T/K)^{E_i}$**

parameter	H ₂ O	BuAc	Bu	HAc
A_i	62.136	59.827	95.577	41.757
B_i	-7258.2	-7285.8	-9914.7	-6304.5
C_i	-7.304	-6.946	-11.768	-4.299
D_i	4.165×10^{-6}	9.990×10^{-18}	1.093×10^{-17}	8.887×10^{-18}
E_i	2.0	6.0	6.0	6.0

complemented with the phase equilibrium data presented above as well as with vapor–liquid equilibrium data for the system 1-butyl acetate + acetic acid measured by Kuranov²¹ in a circulating still (see Table 9). The pure component vapor pressure curves used in the vapor–liquid equilibrium calculations are given in Table 12, and the parameters used to model the dimerization of acetic acid in the vapor phase were taken from Gmehling and Kolbe.²²

Table 13. Binary Parameters α_{ij} and $\tau_{ij} = A_{ij} + (B_{ij})/(T/K)$ of the NRTL Model

component i	H ₂ O	H ₂ O	H ₂ O	BuAc	BuAc	Bu
component j	BuAc	Bu	HAc	Bu	HAc	HAc
A_{ij}	5.563	1.807	-1.667	-1.637	-5.226	-7.338
A_{ji}	-1.677	-1.170	-3.895	-0.167	4.927	5.735
B_{ij}	157.21	628.99	813.48	661.50	2044.38	2797.74
B_{ji}	903.22	682.68	1601.61	222.88	-1801.49	-2268.36
α_{ij}	0.25	0.45	1.7	0.45	0.3	0.3

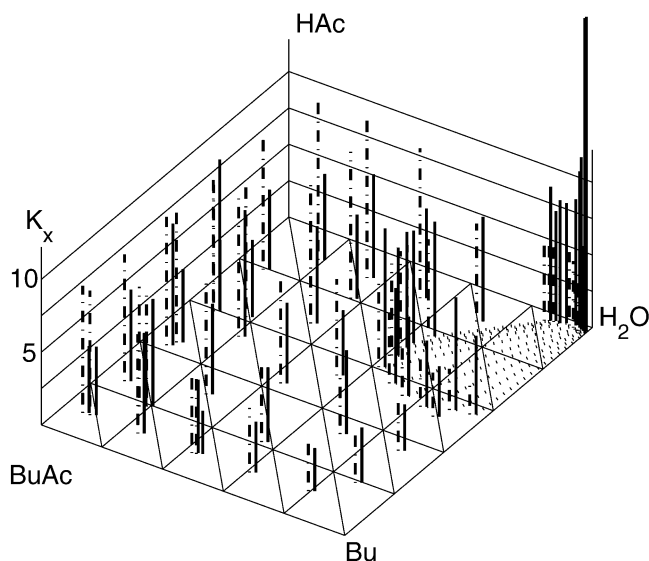
The phase equilibrium models were then used to predict the concentration dependence of the pseudoreaction equilibrium constant in the studied system, and the results were compared to the experimental data from the present work. This paper only summarizes the most important results. For more detailed information, see Grob.¹⁰ In particular, that work gives numbers for average and maximal deviations of the fits of all studied systems (quaternary, ternary, and binary systems) for both vapor–liquid and liquid–liquid equilibrium with all studied models as well as numerical results for the predicted values for K_x and additional graphical representations.

a. NRTL Model. The binary parameters of the NRTL model were fitted to binary, ternary, and quaternary phase equilibrium data. The different experimental data may be weighted in different ways. Thus, different model parameter sets can be obtained. Fitting the parameters to vapor–liquid equilibrium data leads to the best results with regard to reaction equilibrium. For more detailed information, see Grob.¹⁰ The resulting model parameters are given in Table 13. Typical deviations in the prediction of binary vapor–liquid equilibrium are 0.4 K in the temperature and 0.01 mol/mol in the gas phase concentration. For ternary and quaternary mixtures, these deviations increase to average values of 3 K and 0.03 mol/mol. This shows the difficulties in predicting ternary phase equilibrium from binary phase equilibrium data in the studied highly nonideal system. In addition, the prediction of liquid–liquid equilibrium from the model parametrized based only on vapor–liquid equilibrium data leads to relatively high average deviations approaching 0.06 mol/mol. Nevertheless, the NRTL model is able to give good predictions of the concentration dependence of the reaction equilibrium data. The concentration independent activity-based chemical equilibrium constant was determined for each temperature from a fit to the data of the present work using the NRTL model parametrized as described above. The results can be described well by

$$K_a(T) = 2.841 \exp\left(\frac{835.7}{T/K}\right) \quad (8)$$

Figure 8 exemplarily shows the results obtained with the NRTL model at 353.15 K. The trends of K_x along the axes connecting the pure components as well as its absolute values are well predicted. This holds for both the region of homogeneous liquid phase and the miscibility gap. In regions of relatively high experimental uncertainty, the deviations between experiment and prediction are higher than those in the other regions. In the aqueous phase of the miscibility gap, the predicted values of K_x are too low.

b. UNIQUAC Equation. The approach taken using the UNIQUAC model was exactly the same as that for the NRTL model. In particular, the binary parameters of the UNIQUAC equation were fitted to the same data as the parameters of the NRTL equation. Again, fitting the parameters to vapor–liquid equilibrium data leads to the best results concerning reaction equilibrium. For more

**Figure 8.** Reaction equilibria in the system water + 1-butyl acetate + 1-butanol + acetic acid at 353.15 K. Experimental results and prediction from NRTL: —, experimental K_x ; - · -, predicted K_x ; · · · · ·, experimental conodes.**Table 14. Binary Parameters $\tau_{ij} = A_{ij} + (B_{ij})/(T/K)$ of the UNIQUAC Model**

component i	H ₂ O	H ₂ O	H ₂ O	BuAc	BuAc	Bu
component j	BuAc	Bu	HAc	Bu	HAc	HAc
A_{ij}	-0.687	-0.107	0.770	0.608	1.967	-0.651
A_{ji}	0.651	-0.116	1.316	-0.073	-1.278	0.639
B_{ij}	22.09	-230.01	33.82	-327.08	-950.36	-31.89
B_{ji}	-588.35	-5.99	-1074.6	60.29	581.68	-18.15

detailed information, see Grob.¹⁰ The model parameters obtained from this procedure are given in Table 14. The deviations between experimental and predicted phase equilibrium are generally similar to the corresponding deviations of the NRTL model. The thermodynamic reaction equilibrium constant was found to be

$$K_a(T) = 9.882 \exp\left(\frac{440.5}{T/K}\right) \quad (9)$$

Using eq 9 together with the UNIQUAC model with the parameters from Table 14 gives good results for both the absolute values and the trends of the pseudoreaction equilibrium constant, K_x . The predicted values of K_x in the region of limited miscibility in the aqueous phase are again too small. This can be seen exemplarily from Figure 9 for a temperature of 393.15 K.

c. PC-SAFT Equation of State. The pure component parameters of the PC-SAFT model for the four components of interest are given in the literature.^{16,17} Besides the pure component parameters, one parameter per binary subsystem is required. Those parameters were fitted to phase equilibrium data. For more detailed information, see Grob.¹⁰ The zeotropic vapor–liquid equilibrium of the binary system 1-butyl acetate + acetic acid cannot be described using the pure component parameters given in the literature: The variation of the binary parameter always leads to predictions of vapor–liquid equilibria characterized by one or two azeotropes. Therefore, the pure component parameters of 1-butyl acetate were refitted to experimental vapor pressure and liquid density data. It was necessary to model 1-butyl acetate as associating fluid, although this assumption contradicts the experience. The new pure component parameters for 1-butyl acetate are

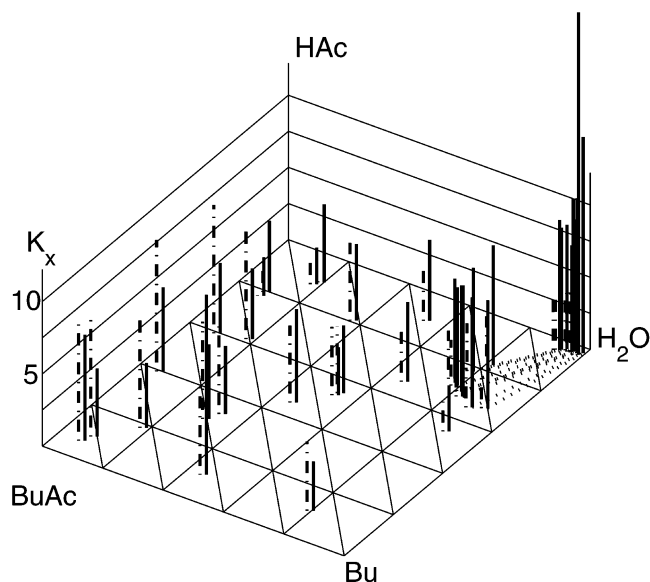


Figure 9. Reaction equilibria in the system water + 1-butyl acetate + 1-butanol + acetic acid at 393.15 K. Experimental results and prediction from UNIQUAC: —, experimental K_x ; - · -, predicted K_x ; · · · · ·, experimental conodes.

Table 15. Pure Component Parameters of the PC-SAFT Equation of State for 1-Butyl Acetate^a

m	2.865
$\sigma/10^{-10}$ m	3.922
$(\epsilon/k_B)/K$	192.33
κ^{AB}	0.2
$(\epsilon^{AB}/k_B)/K$	2261.5

^a m , number of segments of the hard sphere chain; σ , square well diameter; ϵ , square well potential; k_B , Boltzmann's constant; κ^{AB} , effective association volume; and ϵ^{AB} , association energy.

Table 16. Binary Parameters k_{ij} of the PC-SAFT Equation of State

component i	H ₂ O	H ₂ O	H ₂ O	BuAc	BuAc	Bu
component j	BuAc	Bu	HAc	Bu	HAc	HAc
k_{ij}	0.11	0.03	-0.13	0.008	-0.0146	-0.075

given in Table 15. The average relative errors in the vapor pressure and the liquid phase density are 2.24% and 0.27%, respectively, at temperatures between 323 K and 423 K. The pure component parameters for the other three components were taken from the literature (see above). The binary PC-SAFT model parameters fitted in this work are summarized in Table 16. The prediction of phase equilibrium data based on the PC-SAFT equation of state yields higher deviations from the experimental values than that based on the G^E models discussed above. Especially binary phase equilibrium in systems which are not completely miscible is comparatively badly described: The average deviation in the composition concerning vapor–liquid equilibrium of the system water + 1-butyl acetate reaches nearly 0.17 mol/mol.

Fitting the reaction equilibrium constant, K_a , to the experimental data resulted in

$$K_a(T) = 0.748 \exp\left(\frac{1731.0}{T/K}\right) \quad (10)$$

Figure 10 shows exemplarily for a temperature of 373.15 K that most of the trends of K_x are described correctly by the model despite its deficiencies regarding the description of phase equilibria. Compared to the results from the G^E

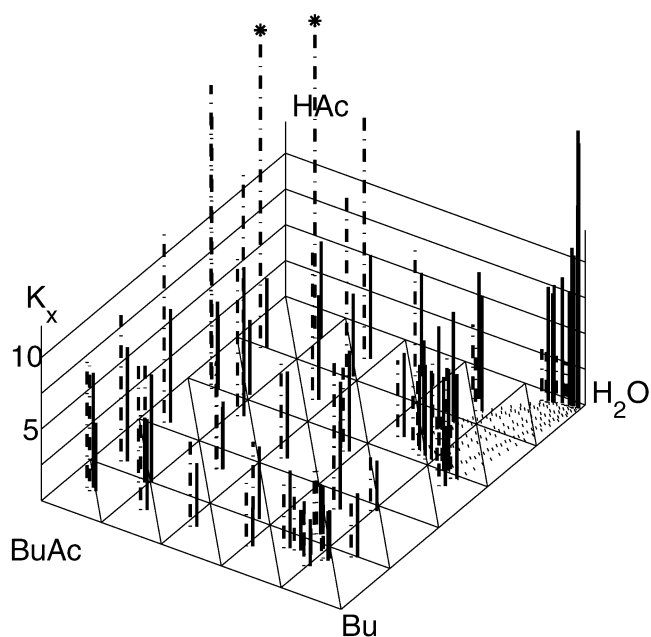


Figure 10. Reaction equilibria in the system water + 1-butyl acetate + 1-butanol + acetic acid at 373.15 K. Experimental results and prediction from PC-SAFT: —, experimental K_x ; - · -, predicted K_x (*, $K_x > 20$); · · · · ·, experimental conodes.

models, the predictions from the PC-SAFT equation of state are of lower quality. In particular, PC-SAFT predicts too high values for K_x in the region of high amounts of acetic acid.

d. COSMO-RS. The COSMO-RS model does not have any parameters which have to be fitted to binary phase equilibrium data. In predictions of binary vapor–liquid equilibrium of the studied systems, the average deviations in the gas phase composition and the temperature are (0.03 to 0.09) mol/mol and (0.7 to 4.6) K, respectively. Especially the binary systems with the miscibility gap are only poorly described, and the prediction of ternary and quaternary vapor–liquid equilibrium data also shows comparatively high deviations from the experimental results. The temperature dependence of the liquid–liquid equilibrium is underestimated. Therefore, the average deviations in predicting liquid–liquid equilibrium are relatively high.

COSMO-RS allows the direct calculation of the pure component Gibbs energy. Thus, the reaction equilibrium constant, K_a , can be obtained directly from COSMO-RS for a given temperature. For reaction I, the results are well described by the following equation:

$$K_a(T) = 98.28 \exp\left(-\frac{535.1}{T/K}\right) \quad (11)$$

It has to be noted that prediction of the weak temperature dependence of K_a with COSMO-RS is qualitatively wrong. Nevertheless, the prediction of the concentration dependence of the reaction equilibrium constant with COSMO-RS gives results which are comparable to those obtained from the other models. Figure 11 shows exemplarily the result for the reaction equilibrium at 353.15 K. The pseudoreaction equilibrium constant predicted for mixtures which are rich in acetic acid takes values which are too high, but concerning the miscibility gap, the composition of the aqueous phase is predicted better than with the other models discussed above. This result shows that COSMO-RS is a promising tool for the prediction of reaction equilibrium, even though the present study has also

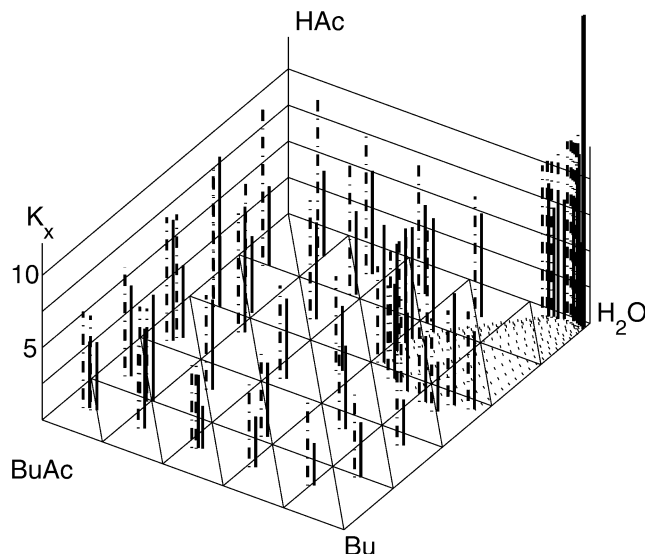


Figure 11. Reaction equilibria in the system water + 1-butyl acetate + 1-butanol + acetic acid at 353.15 K. Experimental results and prediction from COSMO-RS: —, experimental K_x ; - - -, predicted K_x ; ·····, experimental conodes.

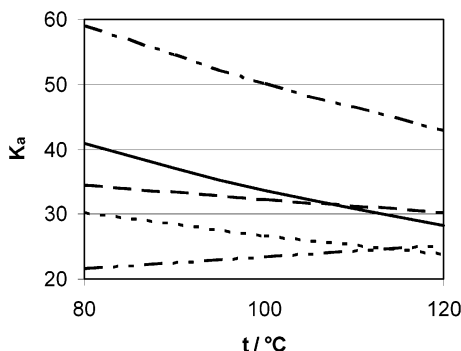


Figure 12. Comparison between K_a calculated from the Gibbs free energy of reaction to K_a fitted to the experimental data of the present work. Models: —, Gibbs free energy of reaction; ·····, NRTL; - - -, UNIQUAC; - · - ·, PC-SAFT; - - - - -, COSMO-RS.

revealed deficiencies of that model in predicting phase equilibria of strongly nonideal systems.

An alternative to fitting the reaction equilibrium constant, K_a , to experimental data is its calculation from the Gibbs free energy of the reaction

$$\Delta_r g^0(T, p) = \mu_{\text{H}_2\text{O}}^{\text{pure}}(T, p) + \mu_{\text{BuAc}}^{\text{pure}}(T, p) - \mu_{\text{Bu}}^{\text{pure}}(T, p) - \mu_{\text{HAc}}^{\text{pure}}(T, p) \quad (12)$$

The pure component chemical potentials, $\mu_i^{\text{pure}}(T, p)$, are available in the literature.²³ Values for K_a calculated from eq 12 are compared to the results from the present work in Figure 12. The result for K_a from the PC-SAFT equation was obtained from K_f using eq 6. The results from eq 12 and from the NRTL and UNIQUAC models show reasonable agreement. The predictions from COSMO-RS lie somewhat lower in the whole temperature range and show the wrong sign of the reaction enthalpy. The results from the PC-SAFT equation lie significantly higher than those from the other models.

Conclusions

On the basis of a comprehensive experimental investigation and literature data, thermodynamic models of both

phase and reaction equilibrium of the esterification system containing acetic acid, 1-butanol, 1-butyl acetate, and water were developed. In contrast to most previous publications on simultaneous modeling of phase and reaction equilibrium, the experiments from the present work on the reaction equilibrium cover the entire composition space including the miscibility gap. The NRTL and UNIQUAC models, the PC-SAFT equation of state, and the COSMO-RS model were studied. The concentration dependence of the Arrhenius mass action law pseudoequilibrium constant, K_x , can be qualitatively predicted over a wide range of the composition space on the basis of phase equilibrium data using any of the models. However, all studied models have difficulties in predicting K_x in regions where the mole fraction of one or more components is comparatively low, in particular, the region of high concentrations of acetic acid and the water-rich phase in the miscibility gap. COSMO-RS allows not only good predictions of the concentration dependence of K_x without using phase equilibrium data but also a prediction of the thermodynamic equilibrium constant, K_a . In the prediction of phase equilibrium, the G^E models which use two or three binary parameters show clear advantages over the PC-SAFT equation of state with only one parameter and the completely predictive COSMO-RS model. Despite this, all models give good results with regard to reaction equilibrium. Especially the COSMO-RS model seems to be promising for predicting the concentration dependence of the pseudoequilibrium constant, K_x .

Acknowledgment

The authors would like to thank R. Dingelstadt, H. H. Fischer, N. Gräber, M. Kapanadze, Y.-K. Kim, M. Maiwald, and P. Matt, University of Stuttgart, who supported experiments which contributed to this work, J. Kuranov, University of St. Petersburg, who provided experiments on vapor-liquid equilibria, and G. Sadowski and F. Tumakaka, University of Dortmund, for supplying the PC-SAFT source code.

Literature Cited

- (1) Hasse, H. Thermodynamics of Reactive Separations. In *Reactive Distillation—Status and Future Directions*; Sundmacher, K., Kienle, A., Eds.; Wiley-VCH: Weinheim, Germany, 2003.
- (2) Lee, L.; Kuo, M. Phase and reaction equilibria of the acetic acid–isopropanol–isopropyl acetate–water system at 760 mmHg. *Fluid Phase Equilibria* **1996**, *123*, 147–165.
- (3) Lee, L.; Liang, S. Phase and reaction equilibria of acetic acid–1-pentanol–water–*n*-amyl acetate system at 760 mmHg. *Fluid Phase Equilibria* **1998**, *149*, 57–74.
- (4) Lee, L.; Lin, R. Reaction and phase equilibria of esterification of isoamyl alcohol and acetic acid at 760 mmHg. *Fluid Phase Equilibria* **1999**, *165*, 261–278.
- (5) Kang, Y. W.; Lee, Y. Y.; Lee, W. K. Vapor-liquid equilibria with chemical reaction equilibrium—systems containing acetic acid, ethyl alcohol, water, and ethyl acetate. *J. Chem. Eng. Jpn.* **1992**, *25* (6), 649–655.
- (6) Leyes, C. E.; Othmer, D. F. Esterification of Butanol and Acetic Acid. *Ind. Eng. Chem.* **1945**, *37*, 968–977.
- (7) Hirata, M.; Komatsu, H. Vapor-Liquid Equilibrium Relation Accompanied with Esterification. *Kagaku Kogaku (Abr. Ed. Engl.)* **1966**, *4*, 242–245.
- (8) Zhuchkov, V. I. Ph.D. Thesis, Moscow Institute of Fine Chemical Technology, Russia, 1986.
- (9) Wendland, M. Hochdruckmehrfasengleichgewichte in ternären Gemischen aus Kohlendioxid, Wasser und einem organischen Lösungsmittel. Ph.D. Thesis, University of Kaiserslautern, Germany, 1994.
- (10) Grob, S. Experimentelle Untersuchung und Modellierung von Reaktion und Phasengleichgewicht am Beispiel des Stoffsystems *n*-Butanol–Essigsäure–*n*-Butylacetat–Wasser. Ph.D. Thesis, University of Stuttgart, Germany, 2004.
- (11) Maiwald, M.; Fischer, H. H.; Ott, M.; Peschla, R.; Kuhnert, C.; Kreiter, C. G.; Maurer, G.; Hasse, H. Quantitative NMR Spectroscopy of Complex Liquid Mixtures: Methods and Results for

- Chemical Equilibria in Formaldehyde–Water–Methanol at Temperatures up to 383 K. *Ind. Eng. Chem. Res.* **2003**, *42*, 259–266.
- (12) Hasse, H. Dampf-Flüssigkeits-Gleichgewichte, Enthalpien und Reaktionskinetik in formaldehydhaltigen Mischungen. Ph.D. Thesis, University of Kaiserslautern, Germany, 1990.
- (13) Ott, M.; Schoemakers, H.; Hasse, H. Distillation of formaldehyde containing mixtures: Experiments, modelling and simulation. Presented at AIChE Spring National Meeting 2003, March 30–April 3, 2003.
- (14) Renon, H.; Prausnitz, J. M. Local Compositions in Thermodynamic Excess Functions for Liquid Mixtures. *AIChE J.* **1968**, *14* (1), 135–144.
- (15) Abrams, D. S.; Prausnitz, J. M. Statistical Thermodynamics of Liquid Mixtures: A New Expression for the Excess Gibbs Energy of Partly or Completely Miscible Systems. *AIChE J.* **1975**, *21* (1), 116–128.
- (16) Gross, J.; Sadowski, G. Perturbed-Chain SAFT: An Equation of State Based on a Perturbation Theory for Chain Molecules. *Ind. Eng. Chem. Res.* **2001**, *40*, 1244–1260.
- (17) Gross, J.; Sadowski, G. Application of the Perturbed-Chain SAFT Equation of State to Associating Systems. *Ind. Eng. Chem. Res.* **2002**, *41*, 5510–5515.
- (18) Eckert, F.; Klamt, A. Fast Solvent Screening via Quantum Chemistry: COSMO-RS Approach. *AIChE J.* **2002**, *48* (2), 369–385.
- (19) Ung, S.; Doherty, M. F. Vapor-liquid-phase equilibrium in systems with multiple chemical reactions. *Chem. Eng. Sci.* **1995**, *50* (1), 23–48.
- (20) Gmehling, J.; Menke, J.; Rarey, J.; Fischer, K.; Cordes, W. *Dortmunder Datenbank. Software: Mixture Properties*, version 1.0.0.168; DDBST Software and Separation Technology GmbH: Industriestrasse 1, D-26121 Oldenburg, 2000.
- (21) Kuranov, G. Vapor-liquid equilibria of the n-butyl acetate–acetic acid system. Private communication, 2002.
- (22) Gmehling, J.; Kolbe, B. *Thermodynamik. 2., überarb. Auflage*; Wiley-VCH: Weinheim, Germany, 1992.
- (23) Poling, B. E.; Prausnitz, J. M.; O'Connell, J. P. *The Properties of Gases and Liquids*, 5th ed.; McGraw-Hill: New York, 2001.

Received for review May 14, 2004. Accepted October 6, 2004. The authors are grateful for the financial support provided by the Deutsche Forschungsgemeinschaft.

JE0498199